Local statistic information-driven active contours for image segmentation

Xiaosheng Yu [1], Qi qi[2], Nan Hu[1]

1. College of Information Science & Engineering, Northeastern University, Shenyang 110819, China
E-mail: yuxiaosheng@ise.neu.edu.cn

2. Shenyang Agricultural University, Shenyang 110866, China
E-mail: 281086154@qq.com

Abstract: This paper presents a local statistic information-driven active contour model for image segmentation. The local intensities of each inhomogeneous object are modeled as Gaussian distributions. The means of Gaussian distributions in each local region are modeled as a bias field multiplying the piecewise constant which reflects the physical property of inhomogeneous objects. A local statistic information fitting energy functional is presented with the level set function, the bias field, the piecewise constant, and variances as variables. The proposed model is implemented by an efficient numerical schema to ensure sufficient numerical accuracy. It is validated on numerous synthetic images and real images, and the promising experimental results show its advantages in terms of robustness and accuracy.

Key Words: Active contour model, image segmentation, bias field, piece constant, level set

1 INTRODUCTION

Image segmentation is a key issue in many pattern recognition applications. In the past decades, many novel image segmentation techniques have been presented, such as the superpixel based methods, the graph cut based methods, and the active contour models [1] based methods. Active contour models have a large number of promising applications, especially in the fields of medical imaging.

The existing active contours models are generally categorized into two types: edge-based models [2-4] and region-based models [5-14]. The former ones usually utilize the boundary information to attract the contours to reach the desired edges. They are applicable to the images which have strong boundaries. However, these models easily suffer from many problems such as serious boundary leakage and high sensitivity to the initial contour and noise, which result in some undesirable effects.

Region-based ones aim to rely on some region-based descriptors to control the contour evolution. They have many advantages in terms of the initial contour localization, the boundary anti-leakage and anti-noise capability over edge-based ones. For example, the famous C-V model has been widely used to segment the binary phase images which are assumed that in each object region the intensities are statistically homogeneous. Therefore, it fails to yield a desired result for the images with intensity inhomogeneity.

There are many methods presented for segmenting objects with intensity inhomogeneity accurately. Wang et al. [7] improved the C-V model by introducing a local term into its energy functional. This method needs to tune a proper weight parameter of the local term for accurate segmentation, but the choice of such a parameter is difficult. Li et al. [8] [9] proposed a local binary fitting (LBF) model, which utilizes the local intensity means, can handle intensity inhomogeneity efficiently. In [10], a local image fitting (LIF) model is presented, which also draws upon the intensity means and can be more efficient than the LBF model with similar capability of dealing with intensity inhomogeneity. Wang et al. [11] proposed a local Gaussian distribution fitting (LGDF) model, which characterizes the local image intensities by Gaussian distributions, can yield results even when serious intensity inhomogeneity exists in the images. Whatever the LBF model, the LIF model and the LGDF model, they only utilize image local region information, which makes them sensitive to the initial contour. In [13], a local intensity clustering (LIC) model is presented. The LIC model relates the local region mean information which is described as a bias field multiplying the true image and thus can efficiently handle intensity inhomogeneity with the flexible location of the initial contour. However, it does not consider the variances in different clusters, which may lead to undesired segmentation.

In this paper, a local statistic information-driven active contour model for image segmentation is presented. We use the local region mean and variance information to construct the local statistic information fitting (LSIF) energy. An efficient numerical schema is used to ensure sufficient numerical accuracy. The experimental results show it can yield a better segmentation.

2 BACKGROUND

2.1 LBF model

Li et al. [8] [9] presented the LBF model to segment images in the presence of intensity inhomogeneity by making use of the local image information efficiently. The LBF model has achieved desired segmentation results. They proposed

This work is supported by National Nature Science Foundation of China (61403068, 61273078, 61203216,61302012) and the Fundamental Research Fund for the Central Universities of China (N140403005, N140404014).

to define the following energy functional

$$E^{\text{LBF}} = \nu\int_{\Omega}\frac{1}{2}(|\nabla\phi|-1)^2\text{d}x+\mu\int_{\Omega}\delta_{\varepsilon}(\phi)|\nabla\phi|\text{d}x$$
$$+\lambda_1\int[\int K(x-y)(I(y)-c_1(x))^2 H_{\varepsilon}(\phi(y))\text{d}y]\text{d}x$$
$$+\lambda_2\int[\int K(x-y)(I(y)-c_2(x))^2(1-H_{\varepsilon}(\phi(y)))\text{d}y]\text{d}x \quad (1)$$

where ν, μ, λ_1, λ_2 are fixed weighting parameters. c_1 and c_2 are two fitting functions that locally approximate the image intensities inside and outside the contour, which enable the LBF model to deal with intensity inhomogeneity efficiently. However, it is only based on the local intensity means, which may cause inaccurate segmentation when the intensity inhomogeneity is strong. Moreover, c_1 and c_2 are only related to the local intensity information, and this may lead to the sensitivity to the initialization of the contour.

2.2 LGDF model

Wang et al. [11] presented the LGDF model to handle the strong intensity inhomogeneity, which aims at describing the local intensities of the image by Guassian distributions. The following energy functional was proposed:

$$E^{\text{LGDF}} = \nu\int_{\Omega}\frac{1}{2}(|\nabla\phi|-1)^2\text{d}x+\mu\int_{\Omega}\delta_{\varepsilon}(\phi)|\nabla\phi|\text{d}x$$
$$-\int[\int K(x-y)\log p_{1,x}(I(y))H_{\varepsilon}(\phi(y))\text{d}y]\text{d}x \quad (2)$$
$$-\int[\int K(x-y)\log p_{2,x}(I(y))(1-H_{\varepsilon}(\phi(y)))\text{d}y]\text{d}x$$

where $P_{i,x}(i=1,2)$ is the probability density function:

$$p_{i,x}(I(y)) = \frac{1}{\sqrt{2\pi}\sigma_i(x)}\exp\left(-\frac{(I(y)-u_i(x))^2}{2\sigma_i(x)^2}\right) \quad (3)$$

where $u_i(x)$ denote the intensity means and $\sigma_i(x)$ denote the standard deviations. It considers both the local region mean and variance information and thus can accurately segment the images with the strong intensity inhomogeneity. However, only the local intensity information is utilized, which may lead to the undesired segmentation without a proper initial contour.

2.3 LIC model

The images with intensity inhomogeneity can be modeled as

$$I = bJ + n \quad (4)$$

where I denotes the given image; b denotes the bias field; J denotes the true signal which is supposed to be piecewise constant; n denotes zero-mean Guassian noise. If the image consists of two regions, foregrounf Ω_1 and background Ω_2, $J(x)=z_i$ for $x\in\Omega_i$, where z_i is a constant, $i=1,2$. Therefore, the local image intensities can be approximated by $b(x)z_i$. Based on this idea, the following energy functional is defined:

$$E^{\text{LIC}} = \nu\int_{\Omega}\frac{1}{2}(|\nabla\phi|-1)^2\text{d}x+\mu\int_{\Omega}\delta_{\varepsilon}(\phi)|\nabla\phi|\text{d}x$$
$$+\int[\int K(x-y)(I(y)-b(x)z_1)^2 H_{\varepsilon}(\phi(y))\text{d}y]\text{d}x \quad (5)$$
$$+\int[\int K(x-y)(I(y)-b(x)z_2)^2(1-H_{\varepsilon}(\phi(y)))\text{d}y]\text{d}x$$

The bias field b is related to the local intensity information, and and are related to the global intensity information. Consequently, the LIC model takes into account the local and global intensity information simultaneously, which enable it deal with intensity inhomogeneity with flexible initialization. However, the LIC model does not consider the local variance, which may make it produce the inaccurate segmentation.

3 THE PROPOSED METHOD

3.1 The formulation of the proposed method

Motivated by the LGDF model and LIC model, we construct a novel method which can be regarded as the combination of these two models. Our model possesses the advantages of the LGDF model and the LIC model that the strong intensity inhomogeneity can be efficiently handled with flexible initialization. Based on the basic frameworks of the LGDF model, we use bz_1 and bz_2 to approximate the intensity means instead of u_1 and u_2, spectively, and define the local statistic information fitting (LSIF) energy:

$$E^{\text{LSIF}} = \int\int_{\Omega_1} -K(x-y)\log p'_{1,x}(I(y))\text{d}y\text{d}x$$
$$+\int\int_{\Omega_2} -K(x-y)\log p'_{2,x}(I(y))\text{d}y\text{d}x \quad (6)$$

where $P'_{i,x}(i=1,2)$ is expressed as:

$$p'_{i,x}(I(y)) = \frac{1}{\sqrt{2\pi}\sigma_i(x)}\exp\left(-\frac{\left(I(y)-b(x)z_i\right)^2}{2\sigma_i(x)^2}\right) \quad (7)$$

The level set function ϕ is able to represent foreground Ω_1 and background Ω_2, inside and outside the zero level set of ϕ, as $\Omega_1=\{\phi>0\}$ and $\Omega_2=\{\phi<0\}$, respectively. Using the level set representation, the E^{LSIF} can be rewritten as

$$E^{LSIF} =$$
$$\int\int K(x-y)(\log(\sqrt{2\pi}\sigma_i(x))+\frac{\left(I(y)-b(x)z_i\right)^2}{2\sigma_i(x)^2})\times$$
$$M_1(\phi(y))dxdy \quad (8)$$
$$+\int\int K(x-y)(\log(\sqrt{2\pi}\sigma_i(x))+\frac{\left(I(y)-b(x)z_i\right)^2}{2\sigma_i(x)^2})\times$$
$$M_2(\phi(y))dxdy$$

where $M_1(\phi(y))=H_{\varepsilon}(\phi(y))$, $M_2(\phi(y))=1-H_{\varepsilon}(\phi(y))$. A length term is often needed to regularize the zero level set of ϕ, which is defined by

$$L(\phi) = \int_{\Omega}|\nabla H_{\varepsilon}(\phi)|\text{d}x = \int_{\Omega}\delta_{\varepsilon}(\phi)|\nabla\phi|\text{d}x \quad (9)$$

The regularized Heaviside function $H_\varepsilon(\phi)$ is commonly expressed as

$$H_\varepsilon(z)=\frac{1}{2}(1+\frac{2}{\pi}\arctan(\frac{z}{\varepsilon})) \tag{10}$$

and the corresponding Dirac function $\delta_\varepsilon(\phi)$ is expressed as

$$\delta_\varepsilon(z)=\frac{1}{\pi}\cdot\frac{\varepsilon}{\varepsilon^2+z^2} \tag{11}$$

The entire energy functional is

$$F^{\mathrm{LSIF}}(\phi,b,z_1,z_2,\sigma_1,\sigma_2)=E^{\mathrm{LSIF}}(\phi,b,z_1,z_2,\sigma_1,\sigma_2)+\mu L(\phi) \tag{12}$$

The regularized Heaviside function $H_\varepsilon(\phi)$ is commonly expressed as

$$H_\varepsilon(z)=\frac{1}{2}(1+\frac{2}{\pi}\arctan(\frac{z}{\varepsilon})) \tag{13}$$

where $\mu>0$ is the weighting parameter.Obviously, if we set $\sigma_1=\sigma_2=1/\sqrt{2\pi}$, our model is as same as the LIC model. However, out model considers the local variances information, which makes it possess better segmentation property than the LIC model.

3.2 The implementation of the proposed method

We use an efficient numerical scheme [15] to implement the proposed method to avoid the re-initialization process. A distance regularizing term is needed to be added in the energy functional. The distance regularizing term is defined by

$$D(\phi)=\int_\Omega\frac{1}{2}(|\nabla\phi|-1)^2dx \tag{14}$$

The energy functional F^{LSIF} in (12) can be rewritten as

$$F^{\mathrm{LSIF}}=E^{\mathrm{LSIF}}(\phi,b,z_1,z_2,\sigma_1,\sigma_2)+\mu L(\phi)+vD(\phi) \tag{15}$$

where v is a nonnegative constant. The segmentation result can be obtained by minimizing this energy functional.

The minimization of F^{LSIF} is able to be realized by using the standard gradient descent method. These variables $\phi,b,z_1,z_2,\sigma_1,\sigma_2$ can be obtained by fixing other variables. By fixing the variables ϕ,b,σ_1,σ_2, and minimizing the energy functional $F^{\mathrm{LSIF}}(\phi,b,z_1,z_2,\sigma_1,\sigma_2)$ with respect to z_1 and z_2, we obtain the closed forms of solutions of z_1 and z_2 as follows

$$z_1=\frac{\int\left(K*\frac{b}{\sigma_1^2}\right)IH_\varepsilon(\phi(y))\mathrm{d}y}{\int\left(K*\frac{b^2}{\sigma_1^2}\right)H_\varepsilon(\phi(y))\mathrm{d}y} \tag{16}$$

$$z_2=\frac{\int\left(K*\frac{b}{\sigma_2^2}\right)I(1-H_\varepsilon(\phi(y)))\mathrm{d}y}{\int\left(K*\frac{b^2}{\sigma_2^2}\right)(1-H_\varepsilon(\phi(y)))\mathrm{d}y} \tag{17}$$

where $*$ denotes the convolution operator.

By fixing the variables $\phi,z_1,z_2,\sigma_1,\sigma_2$ and minimizing the energy functional $F^{\mathrm{LSIF}}(\phi,b,z_1,z_2,\sigma_1,\sigma_2)$ with respect to b, we obtain the minimizer of b as follows

$$b(x)=\frac{\sum_{i=1}^{2}K*(IM_i(\phi(x))\cdot\frac{z_i}{\sigma_i^2(x)}}{\sum_{i=1}^{2}K*M_i(\phi(x))\cdot\frac{z_i^2}{\sigma_i^2(x)}} \tag{18}$$

By fixing the variables ϕ,b,z_1,z_2 and minimizing the energy functional $F^{\mathrm{LSIF}}(\phi,b,z_1,z_2,\sigma_1,\sigma_2)$ with respect to σ_1 and σ_2, we obtain the closed forms of solutions of σ_1 and σ_2 as follows

$$\sigma_1(x)=\sqrt{\frac{\int K(y-x)(I(y)-b(x)z_1)^2M_1(\phi(y))\mathrm{d}y}{\int K(y-x)M_2(\phi(y))\mathrm{d}y}} \tag{19}$$

$$\sigma_2(x)=\sqrt{\frac{\int K(y-x)(I(y)-b(x)z_2)^2M_2(\phi(\mathrm{y}))\mathrm{d}y}{\int K(y-x)M_2(\phi(\mathrm{y}))\mathrm{d}y}} \tag{20}$$

Keeping the variables $b,z_1,z_2,\sigma_1,\sigma_2$ fixed, and minimizing the energy functional $F^{\mathrm{LSIF}}(\phi,b,z_1,z_2,\sigma_1,\sigma_2)$ with respect to ϕ, the corresponding gradient decent flow is:

$$\frac{\partial\phi}{\partial t}=v(\nabla^2\phi-\mathrm{div}(\frac{\nabla\phi}{|\nabla\phi|}))+\mu\delta_\varepsilon(\phi)div(\frac{\nabla\phi}{|\nabla\phi|})-\delta_\varepsilon(\phi)(w_1-w_2) \tag{21}$$

where

$$w_1=\int_\Omega K(y-x)\left(\log(\sigma_1(y))+\frac{(I(x)-b(y)z_1)^2}{2\sigma_1(y)^2}\right)\mathrm{d}y \tag{22}$$

$$w_2=\int_\Omega K(y-x)\left(\log(\sigma_2(y))+\frac{(I(x)-b(y)z_2)^2}{2\sigma_2(y)^2}\right)\mathrm{d}y \tag{23}$$

The procedures can be concluded as follows:

The energy functional F^{LSIF} in (12) can be rewritten as

1. Initialize a level set function as

$$\phi(x)=\begin{cases}-c_0, & x\in R\\ c_0, & \text{otherwise}\end{cases} \tag{24}$$

where c_0 is a positive constant, and R is a region in the image.

2 Initialize the bias field $b=1$, the local standard deviations $\sigma_1=1$ and $\sigma_2=2$.

3.Update z_1 and z_2 using Eqs.(15) and (16), respectively.

4. Update b using Eqs.(17).
5. Update σ_1 using Eqs.(18), and σ_2 using Eqs.(19).
6. Evolve ϕ using Eqs.(20).
7. Return the step 3 until ϕ has converged.

4 EXPERIMENTAL RESULTS

Our model is applied to segment both synthetic and real images of different modalities and compared with the LGDF model and the LIC model, respectively. A truncated Gaussian window K is selected with standard deviation σ. We use the following fixed parameters: $v=1$, $\varepsilon=1$, $c_0=1$, and $\Delta t=0.1$. The parameters μ and σ need to be tuned according to the images.

We utilize the Jaccard similarity (JS) [16] for comparison to quantitatively evaluate the performance of these three models in the experiments. JS can be defined by

$$J(W_1,W_2)=\frac{|W_1 \cap W_2|}{|W_1 \cup W_2|} \tag{25}$$

where W_1 is the segmented object and W_2 is ground truth.

4.1 Comparisons with the LGDF model

Fig.1 and Fig.2 show the comparisons between the LGDF model and our method for segmenting a CT image of heart and a MR image of brain, respectively. The same initial contours are used which are represented by the blue curves in both models. Obviously, the LGDF model fails to segment objects with most initializations because it only considers the local intensity information, as shown in Figure 1(a) and Figure 2(a). Our model takes into account both the local and global intensity information, and thus it always detects the object of interest with different initial contours, as shown in Figure 1(b) and Figure 2(b).

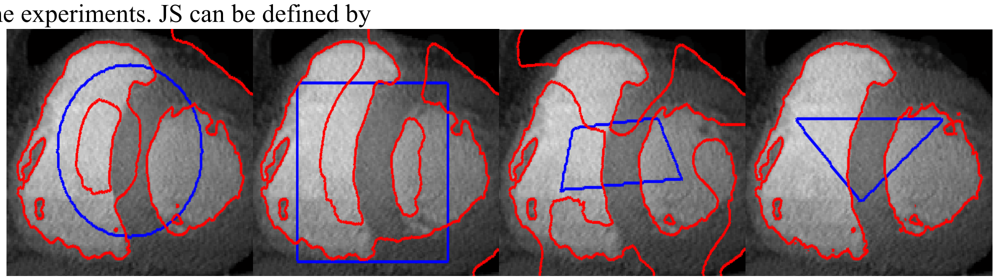

(a) The segmentation results of the LGDF model

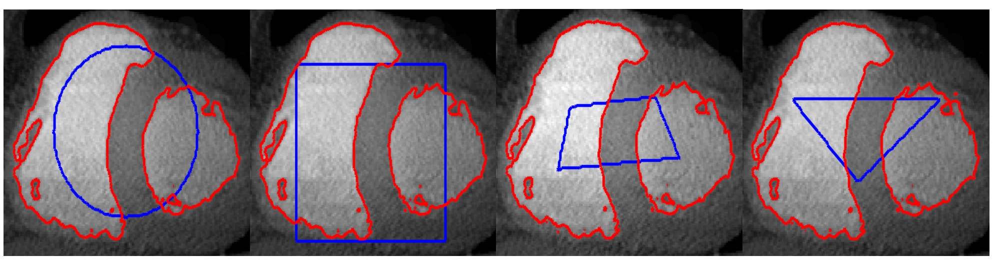

(b)The segmentation results of our model

Fig.1 Performances of the LGDF model and our model on a CT image of heart with different initial contours

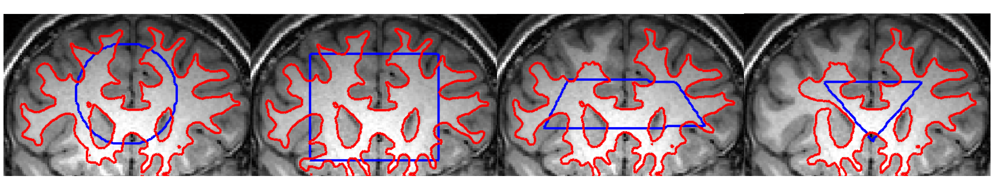

(a) The segmentation results of our model

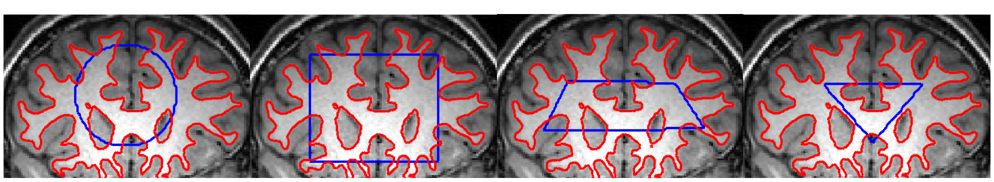

(b)The segmentation results of the LGDF model

Fig.2 Performances of the LGDF model and our model on a MR image of brain with different initial contours

4.2 Comparisons with the LIC model

Fig.3, Fig.4 and Fig.5 show the comparisons between the LIC model and the proposed model for segmenting a synthetic image, an X-ray image of bone and an infrared image of car, respectively. The same initial contours are utilized. Severe intensity inhomogeneity occurs in these three images. Figure 3(b), Figure 4(b) and Figure 5(b) show the segmentation results of the LIC model. Obviously, the LIC model does not work well for them. By contrast, our model can produce much better segmentation results because it considers the local variance information, as shown in Figure 3(c), Figure 4(c) and Figure 5(c). The JS values are shown in Fig. 6. Obviously, our model has better performance.

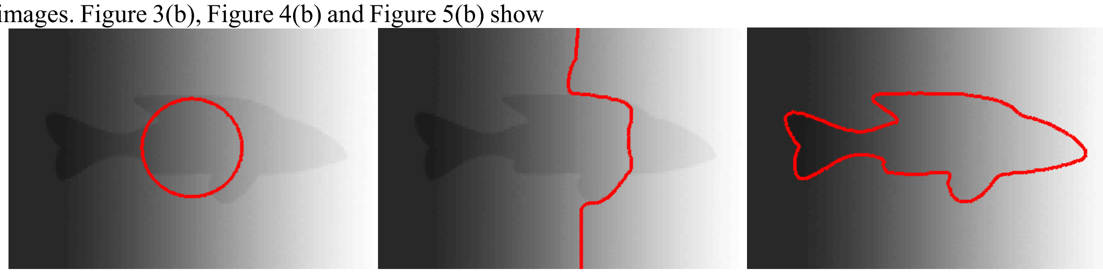

(a) Initial contour (b) LIC model (c) Our model

Fig.3 Comparison of our model with the LIC model in the application to a synthetic image

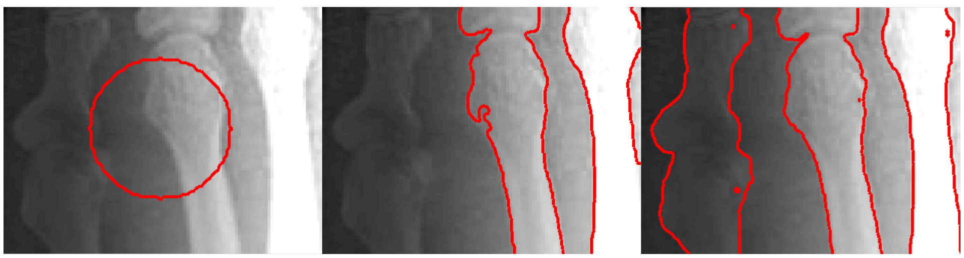

(a) Initial contour (b) LIC model (c) Our model

Fig.4 Comparison of our model with the LIC model in the application to an X-ray image of bone

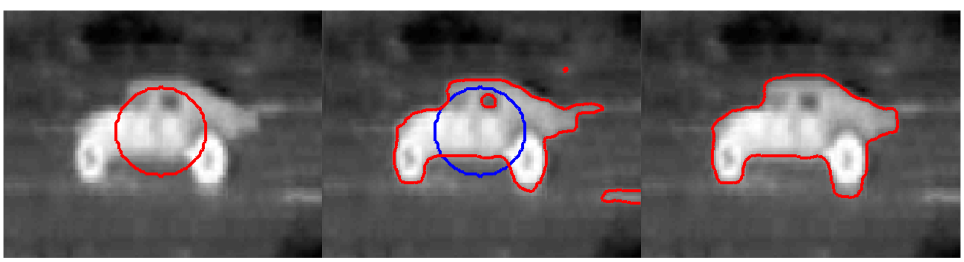

(a) Initial contour (b) LIC model (c) Our model

Fig.5 Comparison of our model with the LIC model in the application to an infrared image of car

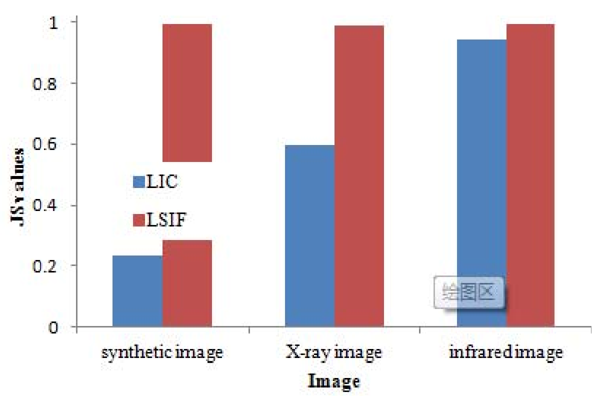

Fig.6 JS values of LIC model and our mode

5 PAPER SUBMISSION

A local statistic information-driven active contour model is presented for image segmentation. Our method utilizes both the local and global statistic information, which makes it more efficient to handle severe intensity inhomogeneity. Our model is also strongly robust to the initial contour. It is implemented with an efficient numerical method in order to ensure the accurate segmentation results and avoid the complex re-initialization procedures. Experiment results demonstrated the advantages of our method in comparison with the LGDF model and LIC model.

REFERENCES

[1] M. Kass, A. Witkin, and D. Terzopoulos, “Snakes: active contour model,” International Journal of Computer Vision, vol.1, pp. 321-331, 1987.

[2] C. Xu, J. Prince, “Snakes, shapes, and gradient vector flow,” IEEE Transactions on Image Processing. vol.7, no.3, pp.359-369, 1998.

[3] V. Caselles, R. Kimmel, and G. Sapiro, “Geodesic active contour models,” International Journal of Computer Vision, vol.1, no.1, pp. 61-79, 1997.

[4] X. Xie, and M. Mirmehdi, “MAC: Magnetostatic active contour model,” IEEE Transactions on Pattern Analysis and Machine Intelligence, vol.30, no.4, pp. 632-647, 2008.

[5] T. Chan, and L. Vese, “Active contours without edges,” IEEE Transactions on Image Processing, vol.10, no.2, pp.266-277, 2001.

[6] L. Vese and T. Chan, “A multiphase level set framework for image segmentation using the mumford and shah model,” International Journal of Computer Vision, vol.50, pp. w271-293, 2002.

[7] X. Wang, D. Huang, and H. Xu, “An efficient local Chan-Vese model for image segmentation,” Pattern Recognition, vol.43, no.3, pp. 603-618, 2010.

[8] C. Li, C. Kao, J. Gore, and Z. Ding, “Implicit active contours driven by local binary fitting energy,” IEEE Conference on Computer Vision and Pattern Recognition, pp. 1-7, 2007.

[9] C. Li , C. Kao, J. Gore, Z. Ding, “Minimization of region-scalable fitting energy for image segmentation,” IEEE Trans-actions on Image Processing, vol.17, no.10, pp. 1940-1949, 2008.

[10] K. Zhang, H. Song, and L. Zhang, “Active contours driven by local image fitting energy,” Pattern Recognition, vol.43, no.4, pp. 1199-1206, 2010.

[11] L. Wang, L. He, A. Mishra and C. Li, “Active contours driven by local Gaussian distribution fitting energy,” Signal Processing, vol.89, no. 12, pp. 2435-2447, 2009.

[12] L. Wang, C. Li, Q. Sun, D. Xia, C. Kao, “Active contours driven by local and global intensity fitting energy with appli-cation to brain MR image segmentation,” Computerized Medical Imaging and Graphics, vol.33, no.7, pp. 520-531, 2009.

[13] C. Li, R. Huang, Z. Ding, J. Gatenby, D. Metaxas and J. Gore, “A level set method for image segmentation in the pres-ence of intensity inhomogeneities with application to MRI,” IEEE Trans. on Image Processing, vol.20, no.7, pp. 2007-2016, 2011.

[14] T. Brox, D. Cremers, “On local region models and a statistical interpretation of the piecewise smooth Mumford-Shah functional,” International Journal of Computer Vision, vol.84, pp. 184-193, 2009.

[15] C. Li, C. Xu, C. Gui, and M. D. Fox, “Level set evolution without re-initialization: A new variational formulation,” Proc. IEEE Conf. Computer Vision and Parattern Recognition, vol.1, pp. 430-436, 2005.

[16] M. Everingham, L. Van Gool, I. Williams, J. Winn and A. Zisserman, “The PASCAL visual object classes (VOC) chal-lenge,” International Journal of Computer Vision, vol.88, no. 2, pp. 303-338, 2010.